

WIYN Bench Upgrade: a revitalized spectrograph

M. Bershad^{*a}, S. Barden^b, P.-A. Blanche^{†c}, D. Blanco^d, C. Corson^{d,e}, S. Crawford^{‡a}, J. Glaspey^d, S. Habraken^c, G. Jacoby^{d,e}, J. Keyes^a, P. Knezek^{d,e}, P. Lemaire^c, M. Liang^d, E. McDougall^{d,e}, G. Poczulp^d, D. Sawyer^d, K. Westfall^a, D. Willmarth^d

^aUniversity of Wisconsin, Department of Astronomy, 475 N Charter St., Madison, WI, USA 53706;

^bAnglo Australia Observatory, PO Box 296, Epping NSW 1710 Australia;

^cCentre Spatial de Liège (CSL), Liège Science Park, Ave. du Pré-Aily, 4031 Angleur, Belgium;

^dNational Optical Astronomical Observatory, 950 N. Cherry Ave., Tucson, AZ, USA 85719;

^eWIYN Observatory, P.O. Box 26732, Tucson, AZ, USA 85726-6732

ABSTRACT

We describe the redesign and upgrade of the versatile fiber-fed Bench Spectrograph on the WIYN 3.5m telescope. The spectrograph is fed by either the Hydra multi-object positioner or integral-field units (IFUs) at two other ports, and can be configured with an adjustable camera-collimator angle to use low-order and echelle gratings. The upgrade, including a new collimator, charge-coupled device (CCD) and modern controller, and volume-phase holographic gratings (VPHG), has high performance-to-cost ratio by combining new technology with a system reconfiguration that optimizes throughput while utilizing as much of the existing instrument as possible. A faster, all-refractive collimator enhances throughput by 60%, nearly eliminates the slit-function due to vignetting, and improves image quality to maintain instrumental resolution. Two VPH gratings deliver twice the diffraction efficiency of existing surface-relief gratings: A 740 l/mm grating (float-glass and post-polished) used in 1st and 2nd-order, and a large 3300 l/mm grating (spectral resolution comparable to the R2 echelle). The combination of collimator, high-quantum efficiency (QE) CCD, and VPH gratings yields throughput gain-factors of up to 3.5.

Keywords: fiber-fed spectrograph design, volume phase holographic grating, CCD performance

1. INTRODUCTION

1.1 History and use

Originally commissioned in the early 1990's for use on the Mayall 4m telescope on Kitt Peak, the Bench Spectrograph¹ was moved to the WIYN 3.5m telescope in 1994 to be used with the Hydra multi-fiber positioner as a first-generation instrument.^{2,3} Two fiber integral-field unit (IFU) feeds were subsequently added: DensePak⁴ in 1997, and SparsePak^{5,6} in 2001. The WIYN Bench Spectrograph and its associated fiber feeds have been a heavily subscribed and a scientifically productive system. In a typical semester the Bench is scheduled for 65% of the science nights, and has been the primary bright-time instrument. Because of its extreme versatility in configuration and feed, this spectrograph system has serviced a wide range of stellar, Galactic and extra-galactic programs.

1.2 Description of salient features

The Bench Spectrograph is fed either by one of two ~100-fiber multi-object bundles (Hydra MOS) patrolling a 1 deg² field, or the 82-fiber SparsePak IFU -- the highest-grasp IFU currently available on any telescope. All are fed at f/6.3 Nasmyth foci. MOS fibers are either 200 μm core low-OH Polymicro FBP-series (1."9, red), or 310 μm, high-OH Polymicro FVP-series (2."9, blue); SparsePak fibers are 500 μm (4."7) ultra-low-OH Polymicro FIP-series, but appear to have transmission properties as good as FIP-STU material.⁷ The recently de-commissioned DensePak IFU used a mix of Polymicro 310 μm fiber types, and was fed both at Nasmyth and the f/13.7 modified-Cassegrain foci (2."9 and 1."3, respectively).

* mab@astro.wisc.edu; phone 1 608 265 3392

† Now at the College of Optical Sciences, The University of Arizona

‡ Now at South African Astronomical Observatories

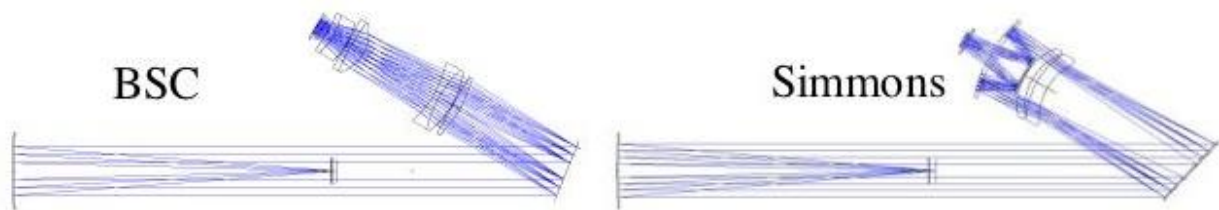


Fig. 1. Optical layouts of the existing Bench Spectrograph system, shown with a low-order grating and 30 deg camera-collimator angle. The all-refractive Bench Spectrograph Camera (BSC) is at left; the catadioptric Simmons camera (two meniscus-lens corrector) is at right. Note the vignetting due to the fiber foot (both cameras), and the added vignetting with the Simmons camera. The spatial waist is located at the fiber feed, about 800 mm before the first turret.

The spectrograph itself is laid out on a 5'x8' optical bench in a passively controlled, closed environment on the ground floor of the observatory. The entrance-aperture consists of a straight, 75 mm pseudo-slit of fibers feeding an on-axis parabolic collimating-mirror of 1021 mm focal length. This system is designed to produce a 152 mm collimated beam from $f/6.7$ fiber output. This design was predicated on the reasonable expectations of the focal-ratio degradation (FRD) due to the fibers and non-telecentricity of the fiber placement at the original Mayall-4m $f/8$ Cassegrain focus. The collimated beam passes back over the fiber feed to a grating turret located about 1800 mm from the collimator, roughly 800 mm beyond the spatial pupil. The turret holds one grating from a suite of six 203x230 mm low-order surface-relief gratings (SRGs; 316 to 1200 l/mm blazed between 4 and 30 deg) and a 206x406 mm R2 echelle (316 l/mm blazed at 63.4 deg) used in single-order mode via order-blocking filters in the fiber feed (see §2.5).

One of two cameras can be configured with an articulating camera-collimator angle between 11-45 deg and a commensurately adjustable camera-grating distance for (single-order) echelle and low-order gratings. These cameras include (1) an all-refractive, all-spherical 8-lens system with 286 mm focal-length and coatings optimized for 450-730 nm; and (2) a catadioptric (Mangin-mirror Maksutov) system with 381 mm focal-length. The latter has a flat 45% throughput due to its central obstruction, and is used in the blue below 380 nm where the refractive camera suffers from greater glass losses or cannot be well focused over broad wavelength coverage. Optical ray-traces with low-order gratings are shown in Figure 1. Both cameras feed a 2048x2048 24 μm pixel SITE CCD. The system delivers instrumental resolutions in the range of $500 < \lambda/\Delta\lambda < 20,000$ between 350 and 950 nm with its suite of fiber feeds.

1.3 Performance, identified problems and solutions

The total system throughput (including telescope and atmosphere) ranges from 3-7% on axis, depending on the specific grating, fiber, and spectrograph configuration; a factor of two lower at the end of the pseudo-slits; and a comparable additional factor at each end of the wavelength range depending on the grating blaze function and camera-grating distance. This inferior performance has been the subject of considerable study and debate, although the field-dependence had long been known to be a vignetting issue associated with poor spatial and spectral pupil placement.⁸

Central to the resolution of the problem was the measurement of the output irradiance of the fibers, illustrated in Figure 2, showing there is considerable power at fiber exit-speeds faster than $f/6.7$ on the WIYN telescope; the scale of FRD when fibers are fed at $f/6.3$ was under-appreciated. Based on these data and a detailed geometric model of the spectrograph we developed our own beam-trace code to understand where losses were occurring in the system (we did not use ZEMAX as this utility does not allow for an arbitrary beam profile, although independent analysis using ZEMAX with a Gaussian beam profile yielded qualitatively similar results). We were able to reproduce the absolute system throughput with reasonable assumptions for surface-losses and grating efficiency, and make detailed matches (better than 10%) to the slit-function and its variation with spectrograph configuration.⁶

On this basis, we concluded that the largest losses in the system were due to vignetting from the combined stops of the fiber entrance-baffle (20% obstruction), the collimator (3-12% undersized), fiber feed (7% obstruction), grating (30-65% over-fill), and camera objective (up to 60% over-fill). Our optical analysis indicated that adopting a 160 mm collimated beam with a reduction of the collimator focal-length to 800 mm would increase system throughput by 40-70%, while minimally degrading spectral resolution with the smallest fibers for which instrumental resolution is limited by optical

aberrations and pixel sampling – points which we quantify in §2.6 and illustrate in Figures 8 and 9. This effective $f/5$ collimator should enclose 90% of the light instead of the 60% enclosed within the 152 mm beam of the current system. Sizing the collimator to allow for a 200 mm beam ($f/4$) would capture most of the 10% remaining signal. An additional gain of 10% could also be achieved by placing the pupil 450 mm beyond the grating location toward the camera. This choice was a compromise between different camera-grating distances between spectrograph configurations, necessary to achieve the spectrograph’s multi-purpose science mission. While this latter gain may seem modest, the throughput improvement for pseudo-slit ends is anticipated to be typically a factor of 2. To consolidate these conceptual optical design gains, the toes need to be shortened and opened to un-obstruct the $f/5$ (or $f/4$) beam, and the foot removed from the optical path via an off-axis or refractive collimator.

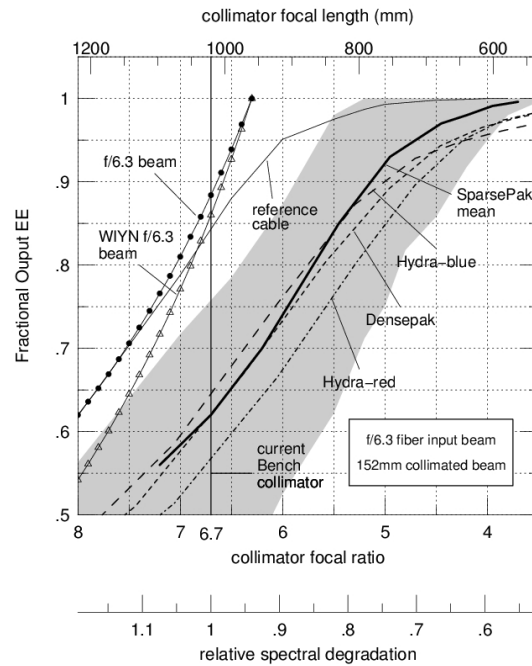


Fig. 2. Fractional output encircled energy (EE) from fibers as a function of WIYN Bench Spectrograph collimator focal ratio (bottom axis) or collimator focal length (top axis). This assumes a 152 mm collimated beam diameter and that all fibers are fed with a $f/6.3$ beam. The current Bench has a $f/6.7$ collimator for a 152mm collimated beam. The mean SparsePak beam profile (thick, solid line), the range for the 13 measured SparsePak fibers (grey shaded area), and reference cable (thin solid curve) are based on laboratory measurements using the $f/6.3$ input beam shown as a thin solid curve with solid circles. Comparable curves, as measured *on the telescope* for DensePak and the two Hydra cables are shown for comparison (private communication, P. Smith & C. Conselice). These measurements use the WIYN $f/6.3$ beam (accounting for the central obstruction), shown as the thin solid curve with open triangles. The very bottom scale (relative spectral degradation) indicates how the spectral resolution of the Bench would alter (worst case) due to changes in system demagnification as a function of changes in the collimator focal length at fixed camera focal length. Actual degradation is substantially less (§2.6) for the smallest fibers. This figure illustrates the effects of FRD on light losses for the Bench Spectrograph, and how optimization trades might be made between throughput and spectral resolution for redesign of the Bench Spectrograph collimator.

Our analysis also indicated that the next most significant gains in system performance would be realized by optimizing the CCD system (higher QE and lower noise), and implementing high diffraction-efficiency volume-phase holographic gratings (VPHGs). The sum of these considerations formed the basis for the Bench Spectrograph Upgrade and framed the requirements of the collimator optical re-design.

2. UPGRADE PROGRAM

The scope of the project was aimed to use as much of the existing system hardware as possible, replacing identified key components to yield performance gains, and modifying relevant interfaces. Kept were fiber feeds, the optical bench, cameras, and grating suite. Replaced were the collimator (§2.1), CCD subsystem (§2.2), and grating turret. Added were a

2nd grating-turret and two VPHGs (§2.3). Modified were the camera-support system and layout (§2.4), fiber-feed interface and focal-surface module (§2.5).

2.1 All-refractive collimator subsystem

The primary challenge in the collimator design was controlling pupil placement and aberrations in a system that could not have a field lens close to the input focal surface due to order-blocking filters sensitive to beam vertex-angle changes. To effect the changes in the collimator described above, the project went through several designs. The designs were optimized for image-quality (rms spot-size at the detector focal surface) over 7 spectrograph configurations with the BSC, and then checked for a Simmons-camera configuration. Configurations included frequently-used gratings modes spanning a broad wavelength range, including 2 low-order gratings (316 and 600 l/mm), three echelle settings (on-order and two off-order), and a folded VPHG mode (see §2.4).

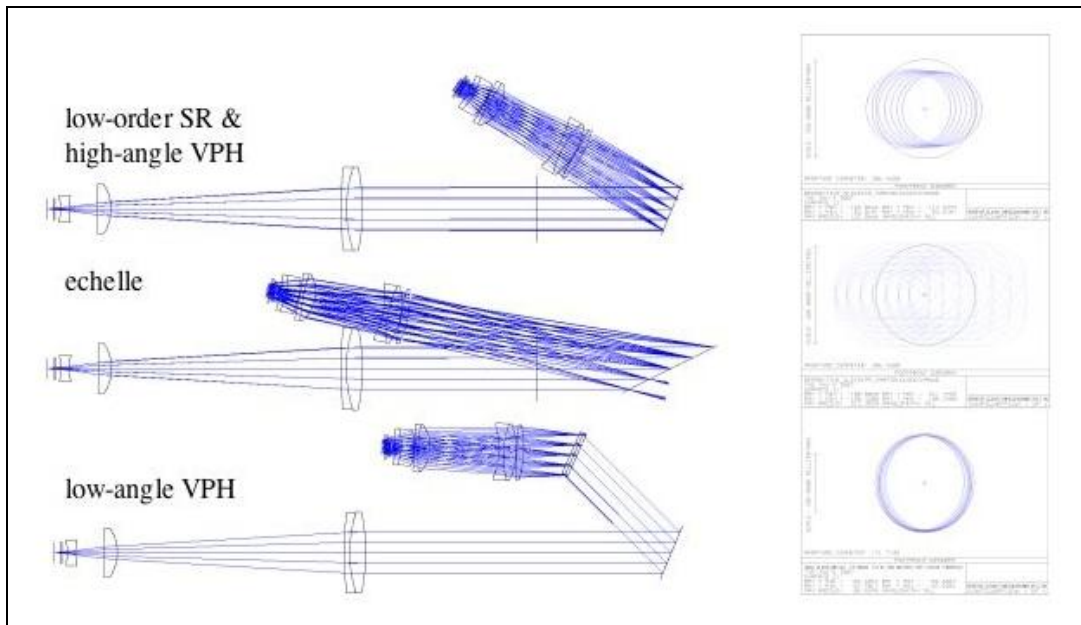


Fig. 3. Optical layout of the Bench Spectrograph with the new all-refractive collimator and the BSC in the three general configurations: low-order surface-relief and high-angle VPH gratings ($\alpha > 35^\circ$; top), echelle (middle), and low-angle VPH ($\alpha < 45^\circ$; bottom). The spatial waist in this system is located 450 mm beyond the first grating turret. At right is shown the beam footprint at the camera-objective.

An initial concept (due to C. Harmer) consisted of an off-axis paraboloid with 4 tilted, all-spherical corrector and field lenses. This novel design achieved most of our requirements, although somewhat degraded image-quality (11%) and did not optimally place the pupil. Most critically, the opto-mechanical tolerances on the tilted-lens system were mechanically difficult to achieve. The project ultimately converged on an all-refractive, on-axis design with 4 all-spherical lenses consisting of two singlets (field-lens and corrector) and a doublet (objective). Ray-traces and layouts of this system are shown in Figure 3 with the BSC for all three primary configurations: (1) low-order SRGs and high-angle VPHGs, (2) echelle, and (3) low-angle folded VPHGs. This design gives good image-quality (3% improvement over existing design), one less surface relative to the off-axis design, and is opto-mechanically straightforward. We added to this optimization a redesigned rear-element (field-flattener) for the BSC and the new, flat CCD device (§2.2). This combination yielded superb image quality of 19 μm (rms) spot-radius on average over the seven spectrograph configurations, 17% better than the current design at $f/5$. Image-quality with an $f/4$ beam is comparable to the existing system. Ghost analysis indicates integrated ghost brightness from all fibers together has a contrast below 10^{-6} , and is dominated by reflections between the last order-blocking filter surface and the first collimator lens surface.

The all-refractive design has all fused-silica (FS) lenses, with the exception of one doublet-lens, which is flint glass (PBL25Y, similar to LF5) for chromatic balance. PBL25Y has above 90% transmission below 350 nm for the designed central thickness. The optics were optimized for $f/5$, but sized for $f/4$, except for a D-shaped cut in the objective

(doublet) to allow the 11-deg camera-collimator angle for echelle configurations. The lost lune still allows $f/4.44$ to pass unvignetted, and minimally obstructs $f/4$; this has inconsequential impact on throughput given the soft beam-profile. To cover the spatial field, the largest element (doublet) has a clear aperture of 320 mm diameter.

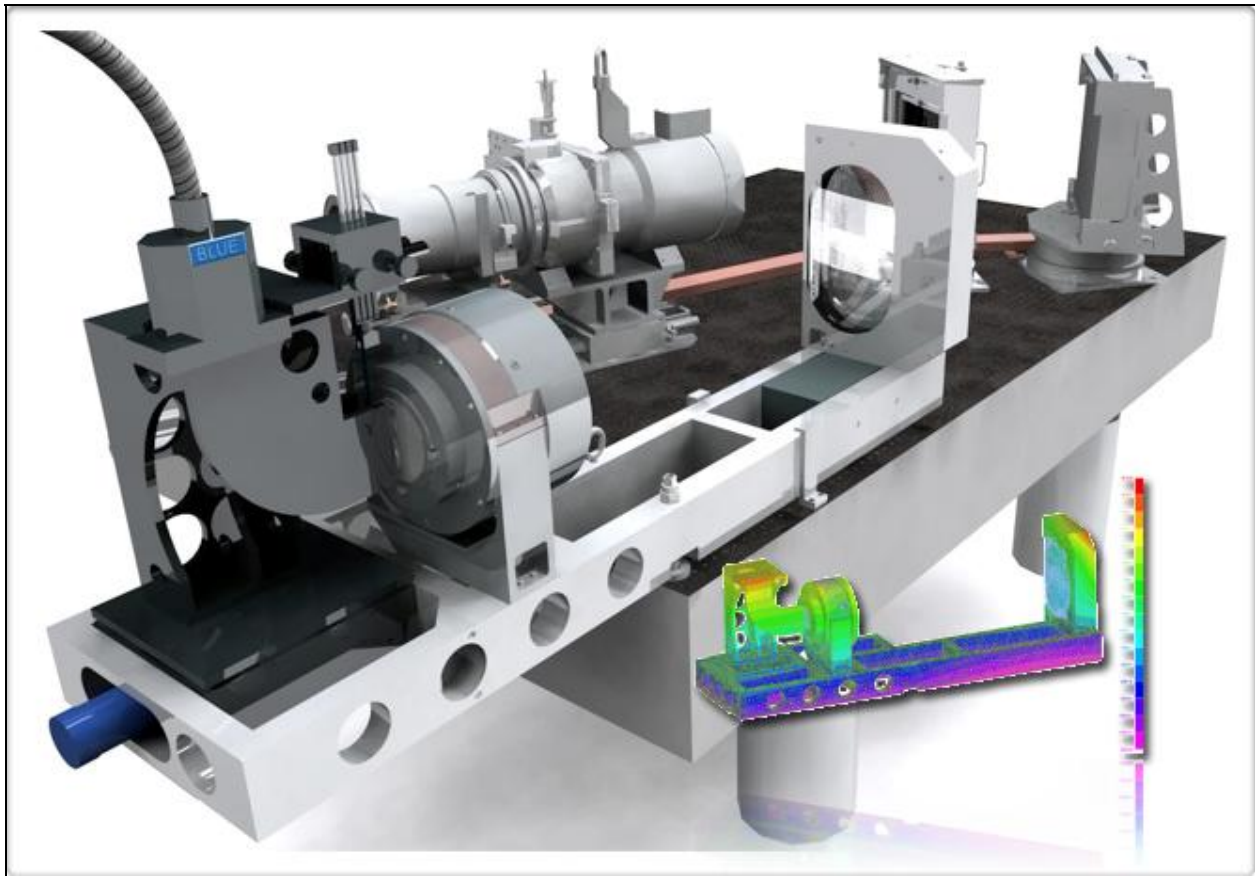


Fig.4. Solid-model of mechanical layout of the upgraded Bench Spectrograph on the existing optical bench, shown in the folded-VPH mode. The all-refractive collimator, housed in two barrels on a sub-bench is at the bottom-left of the table, with the curved fiber feed (foot) at the far left. The focal-surface module (ATV) is behind and obscured by the foot in this vantage. The replaced grating-turret holding a fold flat is at the top-right. A new 2nd grating turret holding the VPHG is behind and to the right of the 2nd collimator barrel (D-shaped, holding the objective doublet). The camera and CCD sub-system on support rails is connected via locating arms to the two turrets. A colored insert shows a finite-element analysis of the collimator sub-system with color scale given 0-0.015 in deflection.

The mechanical design-concept for the collimator is a separate sub-bench that attaches on a semi-kinematic mount to the existing optical bench (Figure 4). The sub-bench is self-contained such that it can be fully assembled, optics internally aligned, tested in the lab, and then delivered as a unit to the spectrograph for direct integration and alignment with the rest of the system. The sub-bench design is structurally rigid enough to allow for cantilevering 700 mm off the table to optimize layout (see §2.4), and integrates the existing fiber-feed module and mount (§2.5). The two singlets are contained in one barrel, with the doublet in a second barrel that contains a manual slide to stop the system down to $f/5$. The entire sub-bench and opto-mechanical assembly were thermally and structurally analyzed, given the known implementation and thermal environment, to achieve the specifications given by the tolerances in the optical design.

The optical fabrication of the collimator was awarded to Société Européenne de Systèmes Optiques (SESO), including the bonding and application of a durable multi-layer anti-reflection coating on the FS-PBL25Y doublet. Coatings are expected to yield $\leq 1.5\%$ losses per surface between 350-950 nm. The two FS singlets, will have a slightly higher-performance coating by Infinite Optics ($\leq 1\%$ per surface in the same range), as will the new BSC rear-element (PBL25Y) and CCD dewar window. Our coating performance requirements were driven by the desire to keep collimator

transmission losses between 350-950 nm at or below the reflection losses (8%) of a freshly coated single Al-coated mirror comparable to the current collimator.

2.2 STA1 CCD sub-system

We have fielded a new CCD sub-system replacing older SITE thinned 2048x2048 24 μm pixel devices (T2KA and T2KC) and associated read-out and control hardware. The new system uses a STA (Semiconductor Technology Associates) 2600x4000 12 μm pixel device (STA1) and MONSOON controller, developed by NOAO, and optimized for low-noise readout. The new format has ample size in the spatial dimension, where typically only 26 mm are required to cover the pseudo-slit; the 2.4% reduction in the spectral-dimension coverage is insignificant, especially considering focus is never good at the edge of the field covered by the current devices. STA1 was a custom-designed CCD for WIYN, made on wafers in a foundry-run to develop orthogonal-transfer CCDs, but is itself a conventional CCD made of low-resistivity silicon. Post-processing, thinning and packaging of the CCD was performed by the University of Arizona's Imaging Technology Lab (ITL) under contract with WIYN. At 160 deg (K) the device has excellent CTE (>99.99996%), and good linearity (0.2% to 10^4 e⁻; 1% to 65×10^4 e⁻). The improved quantum efficiency (QE) of this thinned device (peaking above 90%) delivers 30% throughput gain relative to T2KA, as illustrated in Figure 5.

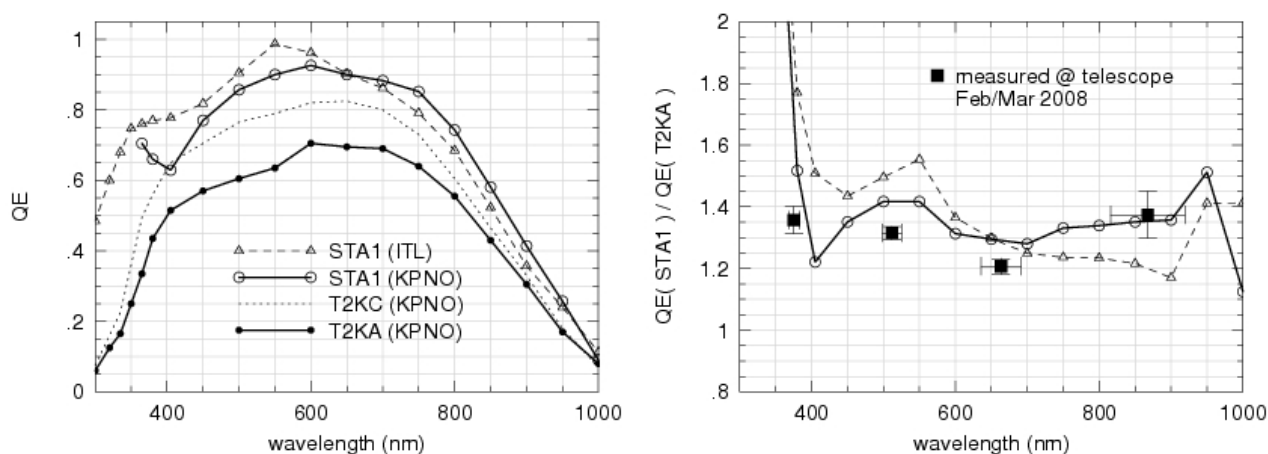


Fig. 5. CCD QE comparison. At left: Lab-measured QE values for the old (T2KA) and new (STA1) CCD systems. Independent measures for STA1 are shown from ITL and KPNO. The original Bench CCD (T2KC) is also shown for reference. At right: The ratio of lab-measured QE for STA1 : T2KA is compared to throughput measurements of these two systems on the Bench spectrograph, all other subsystems fixed (see text). The excellent agreement between lab and in-situ measurements indicates a nearly-constant 30% gain in throughput across wavelength (370-880 nm) with STA1.

The laboratory QE measurements for new and old devices were verified by performing a double-differential measurement on the telescope. This consisted of measuring the flux through 7 fibers spaced evenly across the slit using the red Hydra cable, illuminated with the dome-flat lamps at a known intensity (remaining fibers were masked). Flux measurements were made with the light un-dispersed (a fold-flat replaced the grating) through narrow-band interference filters designed as order-selectors for the echelle; filter central wavelengths ranged from 375-868 nm. Dome-flat measurements with the Mini-Mosaic CCD imager (on the opposite Nasmyth port), through comparable-wavelength narrow and broad-band filters, were interleaved in time with the spectrograph measurements. This experiment was repeated with T2KA and then STA1 with identical spectrograph and imager setups and lamp intensity settings. Our measurements show the dome-lamps at high setting are stable in intensity to better than 1.5% at 550 nm, and stable in color to better than 1% between 370-650 nm over 5 days during a two-month period. This carefully monitored stability allowed us to make an accurate, independent verification of the laboratory QE measurements.

Further advantages of the STA1 CCD system are smaller pixels, faster read-time, and lower read-noise. The smaller pixels are critical for sampling the smallest (200 μm) fibers, which are under-sampled with the 24 μm SITE devices due to the factor of 3.54 system geometric demagnification. This is particularly a problem in the configurations with the highest anamorphic demagnification (under 2 pixels FWHM). This finer sampling, coupled with improved image quality

is a key combination that allows us to maintain and even improve delivered image quality (and hence spectral resolution; §2.6) even while decreasing the collimator focal length.

Detector-noise (rms) and read-time are coupled, both depending on the sampling dwell-time and binning. The initial system release permits binning modes of 1x1, 2x1, 2x2, 4x2, and 4x3 (spatial x spectral) pixels; 2x2 binning delivers equivalent effective pixels as the SITE devices. The larger binning modes are designed for the large SparsePak fibers in the lowest light-level applications. Each of these modes can be sampled at a choice of 3 dwell-times (and corresponding gains), yielding read-times between 18-230 sec. In 2x2 binning mode, read-time are 34-67 sec, which even in the lowest-noise (high-gain, long dwell) sampling is 2.5 times faster than the older controllers used with the SITE devices. The program specification for the detector noise was $\leq 3e^-$ (rms), independent of binning, for the high-gain mode. While the overscan can be as low as 3.4 e^- (rms), the delivered detector noise in bias frames is 3.7 e^- (rms, 1x1 binning) and 4.1 e^- (rms, 2x2 binning). The detector noise varies as a 10% ramp across the device, along with the bias level. The additional source of noise is believed to be due to charge injection from the parallel clocks; the effect has been reduced but not eliminated.

The last remaining issue with the STA1 devices is dark current, which adds significantly to the delivered system noise in long exposures. At 160 deg (K) operating temperature the mean dark count is between 1.3-2 e^- /hr per un-binned pixel, dropping to 0.7 and 0.65 e^- /hr at 155 and 152 deg (K), respectively. At the lowest temperature, there is roughly 5.2 e^- /hr in a 4x2-binned pixel, increasing the detector-limiting noise in the high-gain setting by 25% relative to the 3 e^- (rms) specification. More problematic are roughly 0.2% of the pixels which have very high dark-count of 1200 e^- /hr on average, even at 152 deg (K). These pixels contribute 6-12 events per fiber spectrum. It does appear that the dark current is relatively stable, particularly for the hotter pixels. At time of writing, we are in process of determining the optimum operating temperature (balancing dark-current with QE and CTE), and building a library of dark-frames. Even prior to further optimization, the new STA1 substantially out-performs the earlier CCD subsystem in all significant respects.

2.3 VPHG subsystem

The Bench Upgrade has benefited greatly by a program started by Barden to develop VPHGs for NOAO and the astronomical community.⁹⁻¹¹ We have implemented two Littrow transmission VPHGs initiated by this effort, and developed the capability to field a VPHG suite to augment and replace current SRGs. The two new VPHGs (740 l/mm and 3300 l/mm) were manufactured by CSL. Their technical description and performance are summarized in Figures 6 and 7. Both have remarkable efficiency relative to comparable SRGs (roughly a factor of 2). While the blaze-function of the lower-dispersion grating is more peaked than its SRG counterpart, it has both superb 1st and 2nd-order response. Each of these gratings are unusual: The 740 l/mm VPHG was made on inexpensive float-glass, and post-polished with excellent delivered image-quality. The 3300 l/mm VPHG is one of, if not the largest VPHG made (0.5m in the dispersion dimension), and is designed for peak diffraction efficiency near 60 deg incidence angle (α), with good diffraction efficiency between $50 < \alpha < 70$ deg. In 1st order this grating delivers comparable dispersion to our R2 echelle in order-11 (510 nm central wavelength). We have designed a precision translation mechanism for this grating to compensate for beam displacement due to refraction in the thick substrates; this optimally centers the beam on the dichromated-gelatin of the VPHG.

The outstanding challenge for the VPHG subsystem is to develop high-performance AR coatings for our high-angle grating. Compounding the challenge is the need to apply cold coatings (at temperatures below 100 deg C), and the fact that multi-layer coatings tend to perform better in the blue at larger angles while the VPHG diffraction efficiency shifts to the red. For our 3300 l/mm grating, diffraction efficiency is still excellent at 65 deg, where Fresnel losses are 11% per surface. While we have received several quotes from excellent vendors meeting our specification of 3.5% losses per surface in this angular range, they are best-effort and very high cost (comparable to the grating itself). Resources are unavailable to pursue these bids at this time. It is remarkable that even without coating the 3300 l/mm VPHG is still a factor of two more efficient than our surface-relief echelle (on order) at comparable dispersion.

2.4 Layout: accommodating VPHG and echelle SRG modes

The primary challenge to upgrade implementation was achieving the range of camera-collimator angles needed (1) to take advantage of Littrow VPHG, which tend to have modest blaze-functions at a given angle, but broad super-blaze (see Figures 6 and 7); (2) the desire to achieve a wide range of dispersion with VPHGs (a direct function of camera-collimator angle); and (3) the requirement to field all of our existing SRGs. The latter is constrained most by echelle-grating configurations. By re-designing layout and mounts, on the existing 5'x8' optical bench we will be able to

accommodate all grating configurations, including any VPHG configurations down to 10 deg incidence angles (α) with sufficient camera back-distance to prevent 0th order transmission from entering the camera. VPHG configurations are achieved in one of two modes: (i) a direct mode using the existing grating turret ($\alpha > 35$); or (ii) a folded mode using a Al-coated fold-flat in the existing turret, and a second turret for the VPHG ($\alpha < 45$). Angles as low as 10 deg provide dispersions in the range of our low-order 316, 400, and 600 l/mm surface-relief gratings (at up to twice the efficiency), and are scientifically compelling for, e.g., redshift-survey work and for measuring nebular diagnostics. Lower angles become lossy because of camera over-fill due to the large required back-distance (camera-vignetting) to avoid 0th-order contamination.

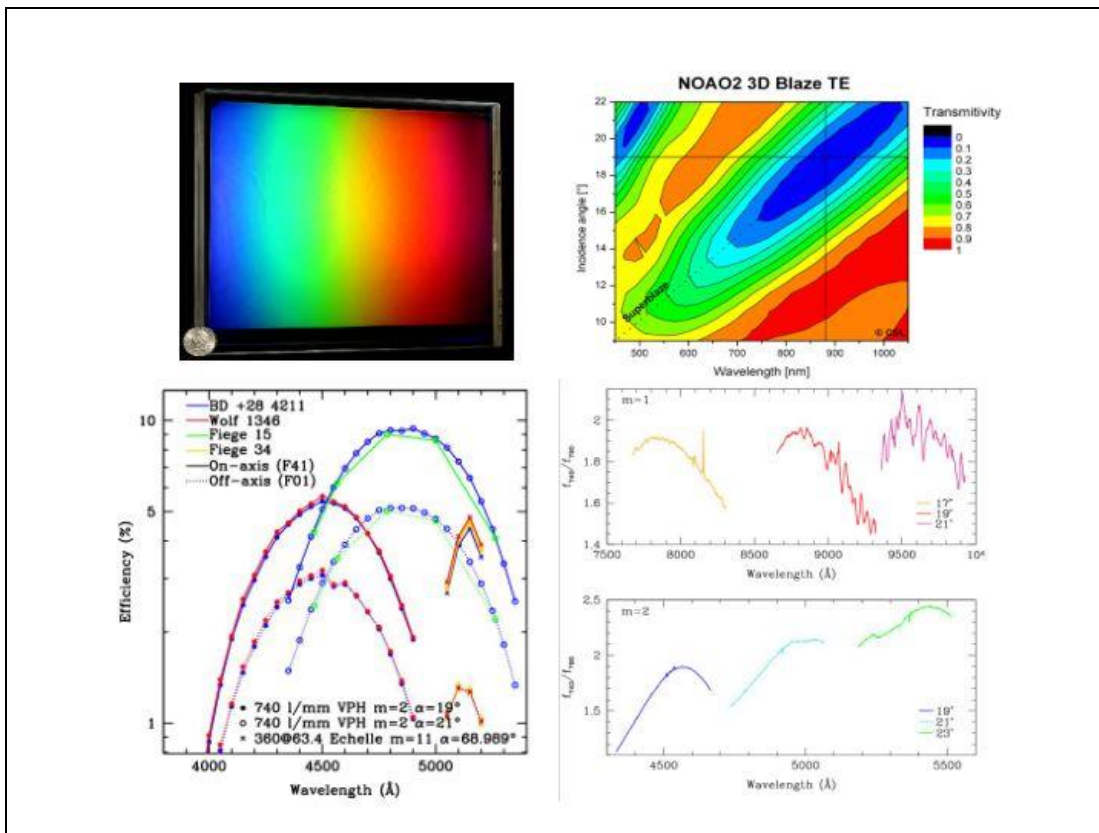


Fig. 6. VPH 740 l/mm grating manufactured by CSL with a clear aperture of 200 x 211.5 mm (physical aperture 220 x 240 mm), an effective gelatin depth of 14 μ m and index modulation of 0.03. This grating was made on Diamant float-glass (12 mm thickness per substrate), post-polished at LLNL to two-dimensional Strehl-ratio of 0.7 in 0th-order transmission and 0.1 for order -1, and coated with a soft MgF₂ at KPNO. Maximum diffraction efficiencies are achieved in m=1 at 880 nm (19 deg) and m=2 peak at 500 nm (21 deg), with blaze-peaks above 80% for 15 $<\alpha<$ 25 deg. In this range the grating delivers spectral resolution between 1000 $<\lambda/\Delta\lambda<$ 4000 for 200-500 micron fibers. On-telescope measurements with the old T2KC CCD using spectro-photometric standards show absolute (bottom left) and relative efficiencies (bottom right) compared to SRGs.

These above two VPHG modes have a 10 deg overlap -- adequate to tune along the super-blaze of any individual grating. To make these all of these configurations possible we (a) modified the support-layout on the camera rails to be more compact and front-loaded; and (b) cantilevered the all-refractive collimator and feed 2' off the table. The latter allowed us to shift the first turret away from its current location at the edge of the bench; this distance sets the lower-limit of the direct mode. We are limited in our movement of the turret not only by the collimator, but also the camera in echelle-mode with 11 deg camera-collimator angles. The latter necessitates long camera-grating distances to un-vignette the incoming collimated beam. Room-enlargement to take a 5'x12' optical bench would permit direct-mode VPHG down to 10 deg. This not only would provide operations-savings in terms of setup and use (the second turret and associated metrology is not motorized), but eliminates the fold-flat (8% gain), and allows for optimum placement of the

camera relative to the pupil (10-15% gain in extreme, low-angle modes). This remains an option for future implementation.

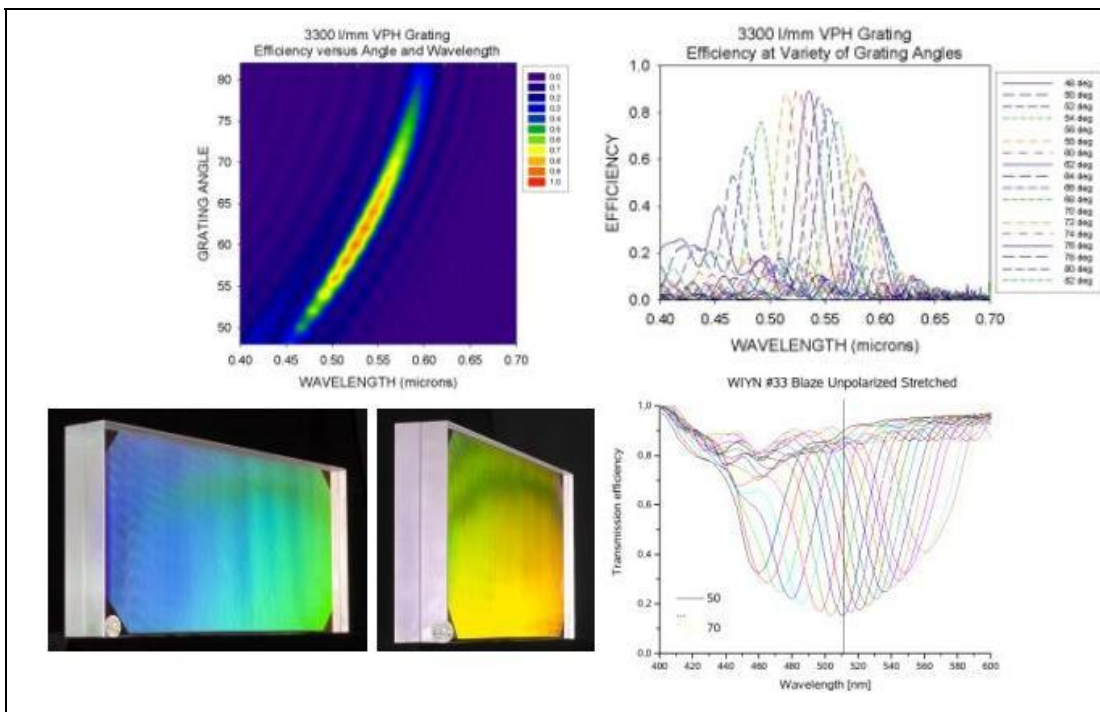


Fig. 7. VPH 3300 l/mm grating manufactured by CSL with a clear aperture of 210 x 480 mm (physical aperture of 230 x 500 mm). Zygo fabricated the two 300 mm thick grating substrates from Corning 7980-2F fused silica. Rigorous coupled-wave predictions of $m=1$ diffraction-efficiency performance are shown in top panels. CSL lab-measurements of 0^{th} order transmission are at bottom. Maximum diffraction efficiency of 85% in $m=1$ is at 57.25 deg (510 nm), with blaze-peaks above 80% for 53-60 deg (485-525 nm), and above 70% for 50-65 deg (465-545 nm). The grating delivers spectral resolution between $4000 < \lambda / \Delta \lambda < 25000$ for 200-500 μm fibers between $45 < \alpha < 70$. Substantial reflection losses exist at these high angles; an advanced AR coating has been pursued but proven too costly to apply at this time. Even without coating the grating outperforms our existing echelle by a factor of 2.

2.5 Focal-surface module (ATV) and fiber feed modifications

This unit consists of a rear-slit viewing camera and an LED fiber back-illuminator, referred together as the ATV. The purpose of this module is to verify target acquisition (via an uncooled CCD camera) and verify positioning at the telescope focal plane (LED rear-illumination). In the current design this system sits on a motorized scissors stage in front of the foot between the foot and the collimating reflector, remotely controlled via a GUI on the data acquisition computer. With the new all-refractive collimator design there is insufficient room between the end of the fiber foot and the first collimator element. We have devised a new scheme for feeding the ATV from the side, by modifying the ends of the fiber feet, known as the “toes.”

The toes contain 4 slots in front of the slit-block which can hold, in order, a slit-mask, a thick (9 mm) interference filter for the echelle, and up to two glass (6 mm) order-blocking filters for the low-order SRGs. Elements for each of these slots are inserted and retracted via motorized slide, and are controlled by a graphical user interface (GUI). There is no use of both smaller filter-slots during observations, so we have eliminated this chamber to allow for more clearance between the removable fiber feed and the first element of the new, all-refractive collimator, and to allow an un-vignetted $f/4$ beam out of the toes. The first (slit-mask) chamber was also unused (anecdotally because it was found not to increase instrumental resolution). This slot has been converted to take a 45 deg fold-mirror to feed the ATV system relocated to a fixed position now to the side of the foot. This required opening a 2 mm wide slit in the side of the toes on one side of this chamber. Very late in the design phase it was reported¹² that Hydra-CTIO Spectrograph users have had recent success achieving higher spectral resolution using slit-masks with the advent of a smaller pixel CCD, not unlike our more-recent upgrade. To ensure we did not lose this capability, we have designed a manual insertion slot for a slit mask

in front of the first slot, and closer to the fiber slit-block. These modifications eliminate two un-necessary actuation mechanisms, retain full ATV functionality, speed-up its insertion, while maintaining and likely improving the capability of increasing spectral resolution via use of a slit-mask.

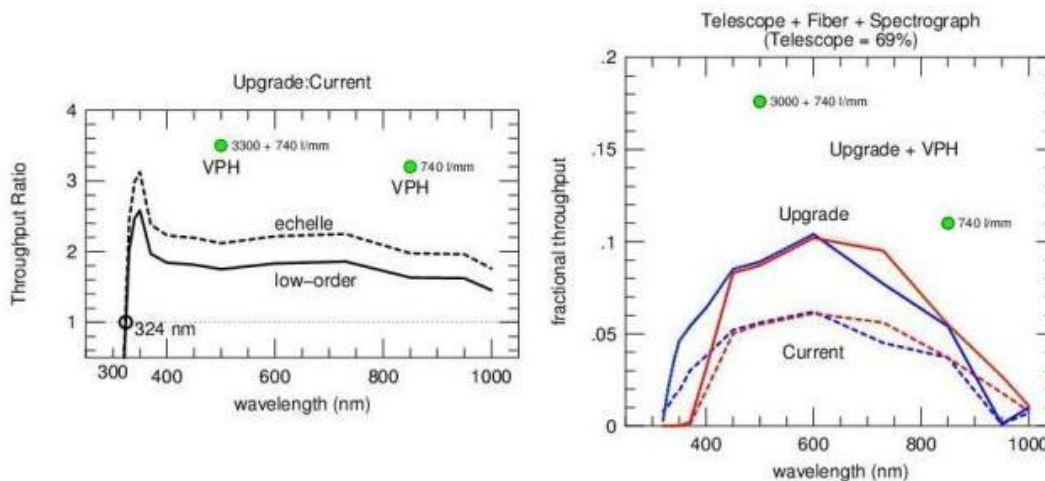


Fig. 8. Expected throughput gains in the upgraded system relative to the current system (left) and in absolute units (right; not including atmosphere, but including 69% telescope throughput for 3 Al surfaces at 88% reflectivity per surface). Red and blue curves are for low- and high-OH fibers (red and blue Hydra) respectively. Gains from VPHG are indicated separately (green points) from other sub-systems gains (feed, collimator and CCD).

2.6 Expected performance gains

Folding together the changes in the feed, collimator, CCD subsystem, and VPHG, we summarize the performance gains in throughput and instrumental (spectral) resolution in Figures 8 and 9, respectively. What is shown are the expectations based on modeling of the post-Critical Design Review planned (upgraded) and existing system. Commissioning efforts are designed and planned to verify these predictions. Example of this verification for the CCD subsystem alone is discussed above in §2.2 (Figure 5) in the context of throughput alone. Overall, throughput gains come also from the modified feed, new collimator and VPHG. The latter contribute both in terms of their superior diffraction efficiency and compact geometry, particularly for high-dispersion (direct) configurations, which in turn minimizes camera vignetting. The all-refractive collimator contributes via a reduced focal length, capturing 40-70% more light into an un-vignetted beam, proper pupil placement (further reducing vignetting), and elimination of the foot obstruction. Losses from added optical surfaces are negated by use of high-performance coatings.

The upgrade perturbs the instrumental resolution by changing the system geometric magnification (28%), improving the image quality due to aberrations (12-20% improvement in the spot-size on average; 30% degradation in one case; and as high as 3x improvement in others), and by improving the detector sampling by a factor of 2. Combined these yield no loss of instrumental resolution on average with the smallest (200 μm) Hydra fibers, 0-15% losses for 300 μm fibers, and 10-20% losses with the 500 μm SparsePak fibers. Of the seven spectrograph configurations we have studied, the two that stand out are the lossy, off-order echelle configuration (image quality is degraded by 25%), and the VPHG configuration (image quality is improved by 35%). These are the outlying points in Figure 9. On balance, this is a desirable trade since the VPHG is a high-throughput configuration.

Overall, the nil to very modest loss of instrumental resolution for substantial throughput gains is the outstanding achievement of the project.

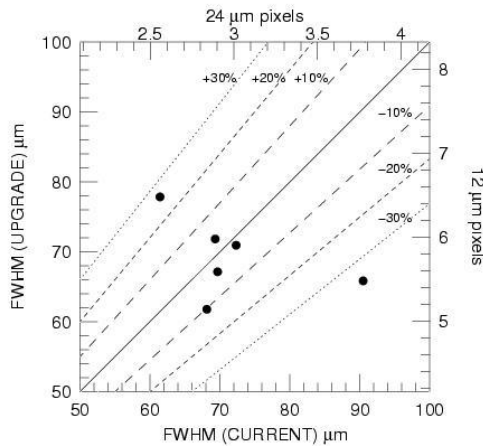


Fig. 9. Expected changes in instrumental resolution, as reckoned by the estimated delivered spectral image-size (FWHM) in the upgraded $f/5$ system versus the existing system using $200\ \mu\text{m}$ fibers. For each of 7 spectrograph configurations, the computation includes the ZEMAX-estimated mean spot-size convolved with the pixel-size and demagnified (geometric and anamorphic) size of the fiber. Since system dispersion is unchanged, the delivered spectral FWHM is directly proportional to resolution. Lines indicate % changes in image-size (negative numbers indicate better instrumental resolution with the upgraded system). Remarkably, on average, there is no instrumental resolution loss with these smallest fibers in the upgraded system, while system throughput increases dramatically.

3. STATUS AND FUTURE PROSPECTS

The upgrade program has currently fielded and completed preliminary commissioning of both VPHGs (folded and direct modes with associated opto-mechanical additions and modifications), and the new STA1 CCD sub-system. Final modifications to the first grating turret to accommodate both SRGs and large VPHGs are underway, and expected to be completed over July/August 2008. Final optimization of STA1 is also anticipated to occur in this time frame. Optical fabrication and coating of the all-refractive collimator optics is underway (all glass is in hand), and is expected to be delivered in mid-August (2008). Collimator opto-mechanical fabrication is complete, awaiting only minor tertiary modifications for as-built measurements of delivered optics. The project is still holding to an aggressive schedule to install, align, laboratory-test the collimator in the second-half of August, and then commission this subsystem (along with associated spectrograph and room layout modifications) in late-August during summer shut-down. With the subsequent analysis and reporting of the final commissioning data, this will complete the Bench Upgrade program.

The upgraded system will afford itself to, and enable, several significant future developments. These include:

- CCD-subsystem: implementation of dual-amp read-out and associated data formatting and reduction software for increased read-out speed.
- VPHG sub-system: (1) development of a full suite of gratings and (2) implementation of a larger optical bench to do away with second turret and fold-mirror.
- Fiber feeds: (1) New IFUs to replace and augment DensePak.¹³ (2) Multi-object IFUs and filtered multi-slit modes for Hydra.¹³ (3) Replacement of current single-fiber MOS system with new Polymicro FBP-series product, revisiting core diameter to re-optimize resolution-throughput product in context of current telescope delivered image quality and fiber-positioning accuracy.

4. SUMMARY

We have described the redesign of the highly-versatile fiber-fed Bench Spectrograph on the WIYN 3.5m telescope. A faster, all-refractive collimator enhances throughput by 60%, on average, by properly matching to the output fiber irradiance (EE90) and optimizing pupil placement. The severe slit-function, which modulated throughput by 50% over

the field, is essentially eliminated. Despite the increase in system magnification, improved optical image quality (achieved by using the collimator design to correct camera aberrations) combined with a new 12 micron pixel CCD maintains or improves the instrumental resolution. Capacity to field VPH gratings permits incidence angles of 10-70 degrees. Two VPH gratings have been manufactured by CSL and are in use. A 740 l/mm grating optimized at 20 deg, made on float-glass and post-polished, delivers twice the system efficiency in 1st and 2nd order relative to a comparable surface-relief grating. A large (0.5m) 3300 l/mm grating delivers spectral resolution in 1st order comparable to the R2 echelle, again at twice the system efficiency -- without coating. Application of an aggressive AR-coating is possible in the future to yield superior performance up to 70 degrees. The combination of collimator, higher QE CCD, and VPH gratings yields efficiency gain-factors up to 3.5 relative to the current system. Improved image quality opens future capabilities to achieve $R = 30,000$ with new, smaller-fiber cables. The all-refractive collimator designs opens the available field for higher spatial multiplex (more fibers), such as multi-object IFUs patrolling a 1 deg^2 field. With improvements and enabled future capabilities from the WIYN Bench Upgrade, we expect to be competitive with a new generation of spectroscopic instruments.

Acknowledgements: This project would not have been possible without the support of the WIYN Board. MAB acknowledges research support from NSF/AST-0607516 and NSF/AST-0804576. We thank James Davies for data-analysis assistance.

REFERENCES

- [1] Barden, S. C., Armandroff, T., Massey, P., Groves, L., Rudeen, A. C., Vaughnn, D., Muller, M., "Hydra – Kitt Peak multi-object spectroscopic system," ed. P. Gray, ASPCS, 37, 185-202 (1993)
- [2] Barden, S. C., Armandroff, T., Muller, G., Rudeen, A. C., Lewis, J., Groves, L. "Modifying Hydra for the WIYN telescope – an optimum telescope, fiber MOS combination," Proc. SPIE, 2198, 87-97 (1994)
- [3] Barden, S. C., Armandroff, T., "The performance of the WIYN fiber-fed MOS system – Hydra," Proc. SPIE, 2476, 56-67 (1995)
- [4] Barden, S. C., Sawyer, D. G., Honeycutt, R. K., "Integral field spectroscopy on the WIYN telescopes using a fiber array," Proc. SPIE, 3355, 892-899 (1998)
- [5] Bershady, M. A., Andersen, D. R., Harker, J., Ramsey, L. W., Verheijen, M. A. W., "SparsePak: a formatted fiber field unit for the WIYN telescope Bench Spectrograph. I. Design, construction, and calibration," PASP, 116, 565-590 (2004)
- [6] Bershady, M. A., Andersen, D. R., Verheijen, M. A. W., Westfall, K. B., Crawford, S. M., Swaters, R. A., "SparsePak: a formatted fiber field unit for the WIYN telescope Bench Spectrograph. II. On-sky performance," ApJS, 156, 311-344 (2005)
- [7] Crause, L., Bershady, M. A., Buckley, D., "Investigation of focal ratio degradation in optical fibres for astronomical application," these Proc. SPIE (2008)
- [8] Vaughnn, D., "Applying information gathering power to the design of a field lens for a high resolution fiber-fed astronomical spectrograph," Masters Thesis, University of Arizona, 1-172 (1994)
- [9] Barden, S. C., Arns, J. A., Colburn, W. S. , "Volume-phase holographic gratings and their potential for astronomical application," Proc. SPIE, 3355, 866-876 (1998)
- [10] Barden, S. C., Arns, J. A., Colburn, W. S., Williams, J. B., "Volume-phase holographic gratings and efficiency of three sample volume-phase holographic gratings," PASP. 112, 809-820 (2000)
- [11] Barden, S. C., Camacho, A., Yarborough, H., "Post-polishing VPH gratings for improved wave-front performance," Proc. SPIE, 4842, 39-42 (2003)
- [12] Frinchaboy, P., private communication (2008)
- [13] Bershady, M. A., Verheijen, M. A. W., Crawford, S. M., " Growth and destruction of disks: Combined HI and HII view," in *Galaxy evolution through the neutral hydrogen window*, eds. R. Minchin and E. Momjian, AIPCS, in press (arXiv:0805.1743v1) (2008)